



HAL
open science

Matching zooplankton abundance and environment in the South Indian Ocean and Southern Ocean

Claire Godet, Marine Robuchon, Boris Leroy, Cédric Cotté, Alberto Baudena,
Ophélie da Silva, Salomé Fabri-Ruiz, Claire Lo Monaco, Sara Sergi, Philippe
Koubbi

► **To cite this version:**

Claire Godet, Marine Robuchon, Boris Leroy, Cédric Cotté, Alberto Baudena, et al.. Matching zooplankton abundance and environment in the South Indian Ocean and Southern Ocean. Deep Sea Research Part I: Oceanographic Research Papers, 2020, 163, pp.103347. 10.1016/j.dsr.2020.103347 . hal-02910918

HAL Id: hal-02910918

<https://hal.science/hal-02910918>

Submitted on 3 Aug 2020

HAL is a multi-disciplinary open access archive for the deposit and dissemination of scientific research documents, whether they are published or not. The documents may come from teaching and research institutions in France or abroad, or from public or private research centers.

L'archive ouverte pluridisciplinaire **HAL**, est destinée au dépôt et à la diffusion de documents scientifiques de niveau recherche, publiés ou non, émanant des établissements d'enseignement et de recherche français ou étrangers, des laboratoires publics ou privés.

1 **Matching zooplankton abundance and environment in the South Indian Ocean and**
2 **Southern Ocean**

3 Claire Godet ¹, Marine Robuchon ^{1,2,3*}, Boris Leroy ¹, Cédric Cotté ⁴, Alberto Baudena ^{4,5},
4 Ophélie Da Silva ^{5,6}, Salomé Fabri-Ruiz ⁵, Claire Lo Monaco ⁴, Sara Sergi ⁴, Philippe Koubbi
5 ^{7,8}

6
7 ¹Laboratoire de biologie des organismes et écosystèmes aquatiques (BOREA), Muséum
8 national d'Histoire naturelle, CNRS, IRD, Sorbonne Université, Université de Caen
9 Normandie, Université des Antilles, CP 26, 57 rue Cuvier 75005 Paris, France

10 ²Centre d'écologie et des sciences de la conservation (CESCO), Muséum national d'Histoire
11 naturelle, CNRS, Sorbonne Université, CP 135, 57 rue Cuvier 75005 Paris, France

12 ³European Commission, Joint Research Centre (JRC), Ispra, Italy

13 ⁴Sorbonne Université UMR 7159 CNRS-IRD-MNHN, LOCEAN-IPSL, 75005 Paris, France

14 ⁵Laboratoire d'Océanographie de Villefranche-sur-Mer, UMR 7093 - CNRS/UPMC - 181
15 Chemin du Lazaret, 06230 Villefranche-sur-Mer Cedex, France

16 ⁶Institut de Systématique, Evolution, Biodiversité (ISYEB), Muséum national d'Histoire
17 naturelle, CNRS, Sorbonne Université, EPHE, Université des Antilles, CP 50, 57 rue Cuvier,
18 75005 Paris, France

19 ⁷UFR918 Terre, Environnement, Biodiversité. Sorbonne Université. 4 place Jussieu, 75252
20 PARIS cedex 05, France

21 ⁸IFREMER Centre Manche Mer du Nord - 150, Quai Gambetta - 62200 Boulogne-sur-Mer,
22 France

23 *Corresponding author: marine.robuchon@ec.europa.eu

24 **Abstract**

25 Distinguishing regions based on the geographic distribution of both abiotic factors and living
26 organisms is an old but still actual central issue for biogeographers. In the Southern Ocean,
27 the few existing regionalization studies have been carried out either at very large scales or on
28 the relatively small region around the Sub-Antarctic islands of Kerguelen and the Crozet
29 archipelagos. However, regionalization studies at meso-scales (100-300 km) covering the
30 Indian part of the Southern Ocean and adjacent South Indian Ocean are scarce. These waters,
31 ranging from the Subtropical to the polar region, are home to large populations of well-
32 studied top predators that depend on the biomass of less known mid-trophic level species such
33 as zooplankton. To fill those gaps, our study aims at conducting bioregional analyses of this
34 transition area at the meso-scale based on the distribution of abiotic factors and chlorophyll-*a*,
35 and to investigate how the abundance of zooplankton varies across the bioregions identified.
36 To that end, we first characterized epipelagic bioregions 30°S in the South Indian Ocean to
37 65°S in the Southern Ocean and from 40° to 85°E including the islands of Crozet, Kerguelen,
38 Saint-Paul and New Amsterdam. We then determined whether these bioregions correspond to
39 variations in the abundance of zooplankton collected by a Continuous Plankton Recorder.
40 Finally, we analyzed which environmental parameters influence zooplankton abundance. Our
41 analyses evidenced six regions, providing a synthetic overview of a contrasting environment.
42 The spatial variability of zooplankton abundance was explained by most of the environmental
43 variables used in the bioregionalisation and, to a lesser extent, by the bioregions. Copepods
44 are abundant in the colder and physically-energetic regions associated with the Antarctic
45 Circumpolar Current (ACC). *Limacina* and euphausiids are both abundant in regions
46 characterized by a high concentration of chlorophyll-*a*, although euphausiids are also abundant
47 in the subtropical region. This work represents a crucial step forward in the integration of
48 living organism distribution in the regionalization of the Indian part of Southern Ocean and

49 adjacent South Indian Ocean. This can, ultimately contribute to the optimization of marine
50 conservation strategies.

51 **Keywords**

52 Bioregionalization, Southern Ocean, Indian Ocean, pelagic ecosystem, zooplankton,

53 Continuous Plankton Recorder

54 1. INTRODUCTION

55 Marine ecoregionalization is a process that aims to divide oceanic areas into distinct spatial
56 regions, using a range of abiotic and biotic – such as chlorophyll-*a* and species assemblages –
57 information (Foster et al, 2017; Hill et al, 2017; Koubbi et al, 2010; Koubbi et al., 2011;
58 Spalding et al., 2007). When data on species assemblages are not sufficiently available to
59 identify ecoregions accurately, bioregions (Grant et al., 2006) or biogeochemical regions
60 (Longhurst, 2010) can be identified based on the distribution of abiotic factors and
61 chlorophyll-*a* only, i.e. available satellite gridded products. The process results in a set of
62 bioregions, each with relatively homogeneous and predictable ecosystem properties (Grant et
63 al., 2006). Bioregions can be divided at different spatial scales, depending on their physical
64 and environmental characteristics. Bioregions are considered as a proxy of biodiversity spatial
65 patterns through an objective zoning. They constitute a basis for understanding, conserving
66 and managing activities in the marine environment (Grant et al., 2006; Ainley et al., 2010;
67 Hogg et al., 2018).

68 Several studies have proposed regionalizations based on the biogeochemical,
69 hydrological or physical and geographical characteristics of the oceans including the Southern
70 Ocean (Grant et al., 2006; Longhurst, 2010; Raymond, 2014; Reygondeau et al., 2014). Four
71 biogeochemical provinces have been identified in the Southern Ocean (Longhurst, 2010) from
72 publications on satellite observations, oceanographic and biotic observations on chlorophyll-
73 *a*, phytoplankton or zooplankton collected during oceanographic surveys. Major changes in
74 these biogeochemical provinces are projected by modeling studies, including southward shifts
75 of the provinces and changes in their areas (Reygondeau et al., 2014). Changes in the
76 Southern Ocean are mainly imputed to the consequences of human activities, both direct
77 (exploitation of living resources by fishing) and indirect (increase in temperature, seasonality
78 of sea ice, ocean acidification; Constable et al., 2014; Turner et al., 2014; IPCC, 2019). These
79 alter the functioning of marine systems and food webs because they induce habitat

80 modifications, which affect primary producers up to top predators, coastal organisms down to
81 deep species, and the Sub-Antarctic Zone up to the sea ice zone (Constable et al., 2014; Gutt
82 et al, 2015).

83 However, the existing Southern Ocean regionalizations (Grant et al., 2006; Raymond,
84 2014) did not consider regional features such as phytoplankton plumes linked to island effects
85 and did not include seasonality. In addition, their northern limit (40°S) excluded the
86 Subtropical zone. This paper proposes to delimit bioregions for the South Indian Ocean and
87 the Southern Ocean covering the area between 40°E and 85°E; 30°S and 65°S. These include
88 the islands of Crozet, Kerguelen, Saint Paul and New Amsterdam. These islands are linked to
89 important topographic features, the ridges of southwest and southeast Indian Del Cano
90 elevation, Crozet Islands' shelf (archipelago) and the Kerguelen Plateau. The occurrence of
91 different water masses and the interaction of the intense ACC with these bathymetric features
92 contribute to the heterogeneity of the region, both from an hydrodynamical point of view and
93 for the subsequent distribution of biogeochemical properties (Roquet et al., 2009; Sokolov
94 and Rintoul, 2007). In this area, the large-scale distribution of primary production and top
95 predators are well known, respectively from remote sensing and biologging data (Cotté et al.,
96 2007; Bost et al., 2009; De Monte et al., 2012; Gandhi et al., 2012; Ropert Coudert et al.,
97 2014). However, very few studies have examined the regional distribution of zooplankton and
98 intermediate trophic levels such as micronekton which includes small organisms (~1–20 cm
99 or g) that can swim (Koubbi, 1993; Handegard et al., 2013; Duhamel et al., 2014; Lehodey et
100 al., 2015; Behagle et al., 2016; Venkataramana et al., 2019). In addition, the main studies on
101 plankton have been mostly conducted in around Kerguelen, either in the coastal zone, above
102 the island shelf or on the eastern edge of the plateau (Blain et al., 2007; Pollard et al., 2007;
103 Sanial et al., 2014).

104 Sampling devices gathering large scale zooplankton information, like the Continuous
105 Plankton Recorder (CPR), can survey vast geographical region to study zooplankton

106 distribution (Batten et al., 2019). This plankton sampling device continuously collects
107 organisms all along a cruise track at the sub-surface and has already been deployed in the
108 Southern Ocean for past studies (Hosie et al., 2003 and 2014). The CPR was deployed for the
109 first time in the South Indian Ocean and the Southern Ocean in 2013 on board the R/V
110 “Marion Dufresne” (Meilland et al., 2016) and since then the surveys have been carried out
111 every year between January and February (Fig. 1). These new samples at high spatial
112 resolution fill a geographic gap in both the South Indian Ocean and the Southern Ocean.

113 Therefore, the objectives of this study were (i) to delimit and characterize bioregions
114 in this area and (ii) to verify whether variations in the abundance of zooplankton can be
115 explained by the environmental characteristics of the bioregions. Specifically, we wanted to
116 define these bioregions at the mesoscale (100-300 km) to provide a better representation of
117 oceanographic features, such as water mass dynamics and fronts. To attain our general
118 objectives, we first delimited summer pelagic bioregions on the basis of environmental
119 parameters (sea surface temperature, chlorophyll-*a* concentration, kinetic energy and
120 bathymetry) describing the main characteristics of the region analyzed. Then, we determined
121 whether these bioregions were precise predictors of variations in zooplankton abundance in
122 the Southern Ocean and the South Indian Ocean by using samples collected by the CPR.
123 Finally, we investigated the extent to which changes in zooplankton abundance were
124 explained by the environmental characteristics of bioregions.

125

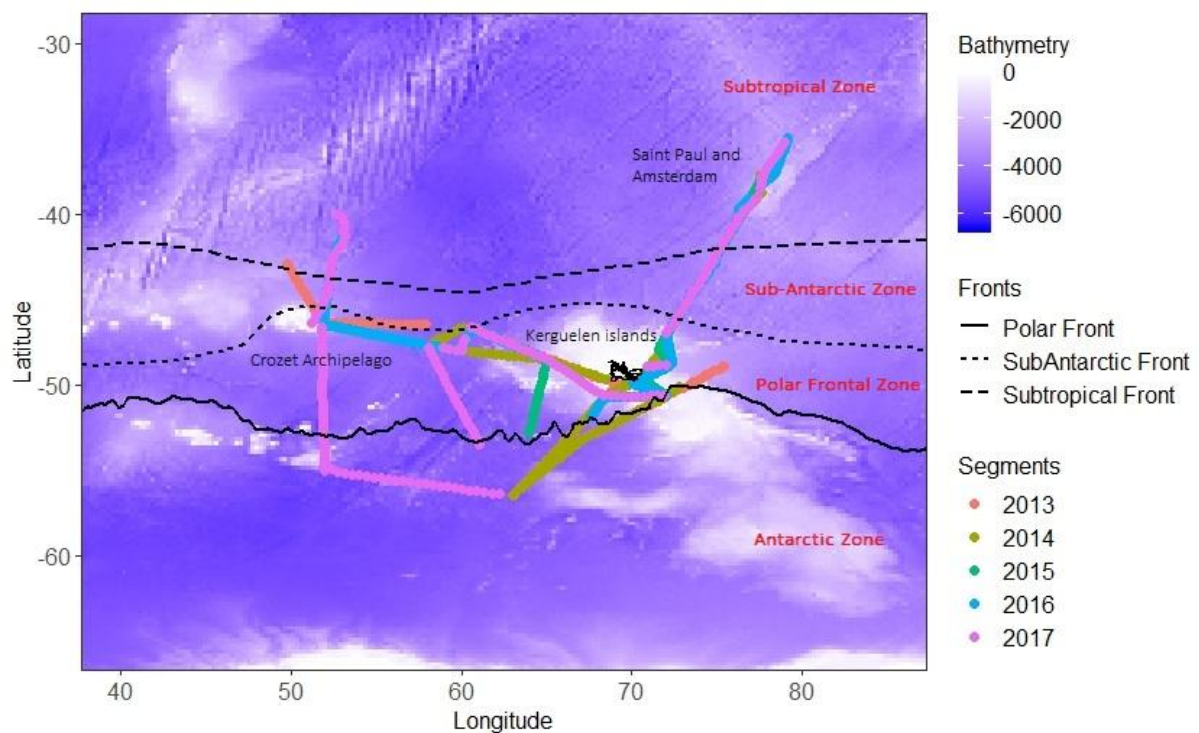
126 **2. MATERIALS AND METHODS**

127 **2.1. Bioregionalization**

128 *2.1.1. Study area*

129 Our study area lies between 40°E and 85°E; 30°S and 65°S (Fig. 1) and includes large
130 latitudinal gradients in water masses properties with different fronts separating the
131 subtropical waters from the polar waters (Orsi et al., 1995). These fronts are associated with
132 the ACC which is very intense in this area. Some of these fronts depict drastic changes in
133 temperature and salinity (Post et al., 2014; Park et al., 1991 and 1993) and delimit large
134 oceanographic regions. The Subtropical Front (STF) defines the southern limit of warm and
135 oligotrophic waters that characterize the subtropical gyre. Further south lies the Sub-Antarctic
136 Front (SAF) associated to the main core of the ACC (Park et al., 2002, 2008), followed by the
137 Antarctic Polar Front (PF). The Sub-Antarctic Zone extends between the STF and the SAF,
138 while the Polar Frontal Zone extends between the SAF and the PF. The Subtropical Zone is
139 located to the north of the STF. In this area, the Sub-Antarctic Zone corresponds to a narrow
140 band of about 2° of latitude (between 44°S and 46°S) that is formed by the convergence of the
141 SAF and STF, in the East of the Kerguelen shelf the PF is also close to the other fronts (Park
142 et al., 1991 and 1993). The largest extent of the Polar Frontal Zone is found to the south of
143 Crozet (between 45°S and 52°S), while it covers only a few degrees in latitude to the north-
144 east of Kerguelen (Sokolov and Rintoul, 2009). The Subtropical Zone also includes the
145 Agulhas Return Current, current which influences species assemblages in the western
146 subtropical part of the area (Koubbi, 1993). On a longitudinal scale, several shallow island
147 shelves and seamounts diversify the geomorphological landscape and shape the ocean
148 circulation. The Kerguelen plateau is a major bathymetric feature extending from the
149 Kerguelen island shelf towards the Antarctic shelf. It deeply, influences the hydrology of the
150 area. It acts as a barrier deflecting the ACC which flows continuously through the Southern
151 Ocean due to the absence of continental lands (Roquet et al., 2009). The study area is also
152 highly heterogeneous in terms of biological productivity. Most of the ice-free polar waters in
153 the Permanent Open Ocean Zone (zone between 50° and 60°S; Pondaven et al., 1998) are
154 characterized by High Nutrient Low Chlorophyll (HNLC; i.e. phytoplankton are not abundant

155 whereas there are high macronutrient levels) conditions due to iron limitation. This trace
 156 element limits the primary production in the study area (Martin, 1990; De Baar et al., 1995).
 157 The HNLC region contrasts with the intense phytoplankton blooms occurring close to iron
 158 sources, notably around the Sub-Antarctic islands. There, the iron is delivered by the
 159 interaction of the flow and the shallow topography (Boyd and Ellwood, 2010). This physical
 160 and biogeochemical process supports recurrent phytoplankton blooms, occurring during
 161 spring over the plateau between Kerguelen and Heard Islands (southeast of Kerguelen), north
 162 and east of Kerguelen (Blain et al., 2007; Park et al., 2008), as well as north and east of
 163 Crozet (Pollard et al., 2007; Sanial et al., 2014). Conversely, the upstream waters of
 164 Kerguelen and Crozet are generally less productive.



165
 166 **Fig. 1.** Map of the study area showing the routes of the oceanographic vessel for each year
 167 (2013-2017), the different fronts of the represented area (Subtropical Front, Sub-Antarctic
 168 Front and Polar Front) and the different zones of the area (Subtropical Zone, Sub-Antarctic

169 Zone , Polar Frontal Zone and Antarctic Zone). The position of the fronts follows Park et al.
 170 (2014).

171 *2.1.2. Environmental data*

172 Our first objective was to delineate bioregions on the basis of four environmental parameters:
 173 (i) sea surface temperature, which varies latitudinally in the study area, (ii) chlorophyll-*a*
 174 concentration, which is an indicator of phytoplankton abundance and iron enrichment zones,
 175 (iii) kinetic energy, which identifies physically-energetic zones associated with the ACC and
 176 (iv) bathymetry, which distinguish shelf from open ocean zones.

177 Oceanographic data were obtained from satellite measurements from 2013 to 2017 for
 178 the period from November to March (i.e. during Austral summer). The parameters studied
 179 were sea surface temperature (SST, in °C), chlorophyll-*a* concentration (Chl-*a*, in mg.m-3),
 180 kinetic energy (KE, in m².s-2) and bathymetry (Bat, in m) (Table 1). Each environmental
 181 parameter had a different spatial resolution. In order to manage these differences, we carried
 182 out bioregionalization at the lowest resolution of the environmental parameters, i.e. the spatial
 183 resolution of the kinetic energy at 0.25°.

184 **Table 1.** Description of environmental parameters used in this study

Environmental parameters	Abbreviations	Source and products	Spatial Resolution	Daily resolution
[Chlorophyll- <i>a</i>] (mg.m-3)	Chl- <i>a</i>	Copernicus Marine Environmental Monitoring Service website (http://marine.copernicus.eu/): "OCEANCOLOUR_GLO_CHL_L4_REP_OBSERVATIONS_009_082" for 2013 and 2014 data and "OCEANCOLOUR_GLO_CHL_L4_NRT_OBSERVATIONS_009_033" (satellite products).	0.04°	8 days mean
Sea Surface	SST	Copernicus Marine Environmental Monitoring Service	0.05°	Daily

Temperature (°C)		website (http://marine.copernicus.eu/): "SST_GLO_SST_L4_NRT_OBSERVATIONS_010_001" (satellite products).		mean
Kinetic Energy (m ² .s ⁻²).	KE	KE data were obtained from the zonal and southern velocity (U and V, respectively) which estimate surface currents derived from altimetry through a geostrophic approximation. U and V are provided in the 'SEALEVEL_GLO_PHY_L4_REP_OBSERVATIONS_08_047' product which was downloaded from the E.U. Copernicus Marine Environment Monitoring Service (CMEMS, http://marine.copernicus.eu/ for the period 2013-2017. In this way, an estimation of the total kinetic energy is obtained.	0.25°	Daily mean
Bathymetry (m)	Bat	http://www.gebco.net (satellite products)	0.008°	/

185

186 The KE was calculated from the altimetry-based horizontal current velocities, using
187 the following formula:

188
$$KE = 0.5 \cdot (U^2 + V^2) / 1000,$$

189 where U and V are the zonal (i.e. longitude) and meridional (i.e. latitude) velocities. The
190 bathymetry of the study area was downloaded from the General Bathymetric Chart of the
191 Oceans website (www.gebco.net).

192 Oceanographic data were downloaded for the period November to March for the years
193 2013, 2014, 2015, 2016 and 2017. The raw data correspond to daily averages for the SST and
194 KE parameters and weekly averages for the Chl-*a* parameter, due to the very high cloud cover
195 in the study area. Data were then analyzed using the mean value calculated over the summer
196 period (November to March).

197 2.1.3. Zooplankton sampling and identification

198 Zooplankton was sampled using a CPR on board the R/V “Marion Dufresne” every summer,
199 between January and February, from 2013 to 2017, for a total of 1282 samples corresponding
200 to 6410 nautical miles. The CPR is a mechanical device that allows continuous sampling of
201 plankton while being towed in the subsurface behind the vessel (at a speed from 10 to 15
202 knots). The CPR was towed approximately 100 m behind the vessel at a depth varying
203 between 10 and 30 m. The CPR works as follows: water enters through a square opening
204 (1.62 cm²: 1.27x1.27 cm) into a collecting tunnel (10x5 cm). The plankton then reaches a
205 moving silk band (filter silk) with an average mesh size of 270 µm. A second strip of silk
206 (covering silk) covers the filtering silk and is then wound in the fixing tank, which contains
207 diluted formaldehyde. Regardless of the speed of the vessel, the silk advances at a speed of
208 about 1 cm per nautical mile during towing (Hunt and Hosie, 2003; Hosie et al., 2014).

209 In the laboratory, each set of silk is unwound and cut by segments of 5 nautical miles.
210 The entire content of each sample is identified at a coarse taxonomic resolution and assigned
211 to one of the following groups: copepods, euphausiids, amphipods, *Limacina*, chaetognaths
212 and ostracods, which are counted under a stereomicroscope. For each major taxon, the
213 individuals are counted in the fraction where at least 100 individuals of that taxon are found.
214 For this a Folsom splitter was used.

215 Zooplankton abundance data obtained by the CPR (2013-2017) for each taxon and silk
216 sample and the corresponding metadata (GPS coordinates) were stored in a table. The
217 abundances were calculated (number of individuals per nautical mile) and each sample was
218 assigned to the time of day (Day, Dusk, Night, Dawn) which was calculated using the solar
219 angle ("RAtmosphere" package; Biavati, 2014). The number of samples is 552 during the day,
220 167 at dusk, 338 at night and 225 at dawn.

221 2.2. Data processing and statistical analyses

222 All statistical analyses were done using R (R Core Team, 2018) and the maps were realized
223 using either R or using a Geographic Information System (ArcGIS v. 10.5.1).

224 *2.2.1. Bioregionalization*

225 The first step in the bioregionalization procedure was to conduct a principal component
226 analysis (PCA, Legendre and Legendre, package “FactoMineR”, 1998; Lê et al., 2008) on
227 environmental parameters (SST, KE, Bat and Chl-*a*) to eliminate noise before classification
228 (concentration of information on the first components), resulting in a more stable
229 classification. The second step consisted of clustering sites by applying the method of K-
230 means (MacQueen, 1967) on the coordinates of site on the two first PCA axes. The optimal
231 number of clusters (in this study, the environmental envelopes of bioregions) was chosen
232 using the index of Calinski Harabasz (1974) and the elbow method (NG, 2012). The final step
233 was to create a map of bioregions based on the clusters obtained.

234 235 *2.2.2. Characterization of zooplankton sampling*

236 To study variations in zooplankton abundance ($\log(\text{abundance}+1)$) between the different taxa,
237 a Kruskal-Wallis analysis was conducted. The same analysis was performed without zero
238 values of abundance for each taxon, to take into account the fact that some taxa live in schools
239 in the Southern Ocean. After each Kruskal-Wallis analysis, post-hoc pairwise Wilcoxon rank
240 sum tests were carried out. This consisted of a multiple comparison test with correction by the
241 Holm method (1979) between each pair of taxa to unravel the differences between them.

242 *2.2.3. Analyses of variation in plankton abundance*

243 The following analyses were carried out on the total abundance of zooplankton (including
244 data with zero values). To investigate how zooplankton abundance ($\log(\text{abundance}+1)$) varied
245 according to the period of the day, a Kruskal-Wallis analysis was performed. The same
246 analysis was performed to test differences in abundances between years. Post-hoc pairwise

247 Wilcoxon rank sum tests were also carried out to unravel the differences between each pair of
248 periods of the day.

249 These analyses focused on copepods, euphausiids and *Limacina*, which were the most
250 abundant taxa. Night samples were used for this analysis because at night, zooplankton
251 abundance and diversity are higher due to nocturnal migrations. A Kruskal-Wallis test was
252 used to study variations in the abundance of copepods, euphausiids and *Limacina* between the
253 different bioregions. A Kruskal-Wallis test was used to study variations in the abundance of
254 copepods, euphausiids and *Limacina* in the different bioregions. Subsequent post-hoc pairwise
255 Wilcoxon rank sum tests were carried out to reveal the differences between each pair of
256 bioregions regarding the abundance of each taxon. Then, a generalized linear model (with
257 Poisson distribution) was used to study the fluctuations in the abundance of the different taxa
258 as a function of different environmental parameters (SST, the log of KE, the log of Chl-*a* and
259 the log of Bat).

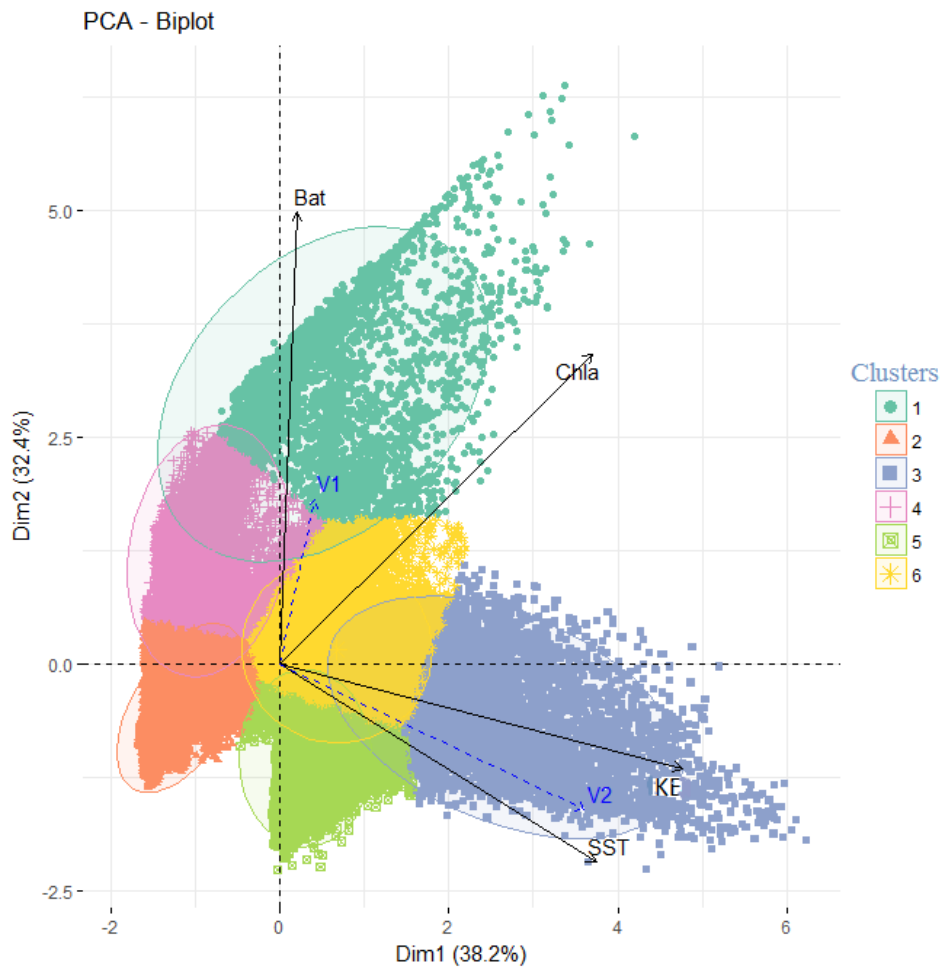
260

261 **3. RESULTS**

262 **3.1. Characterization of bioregions**

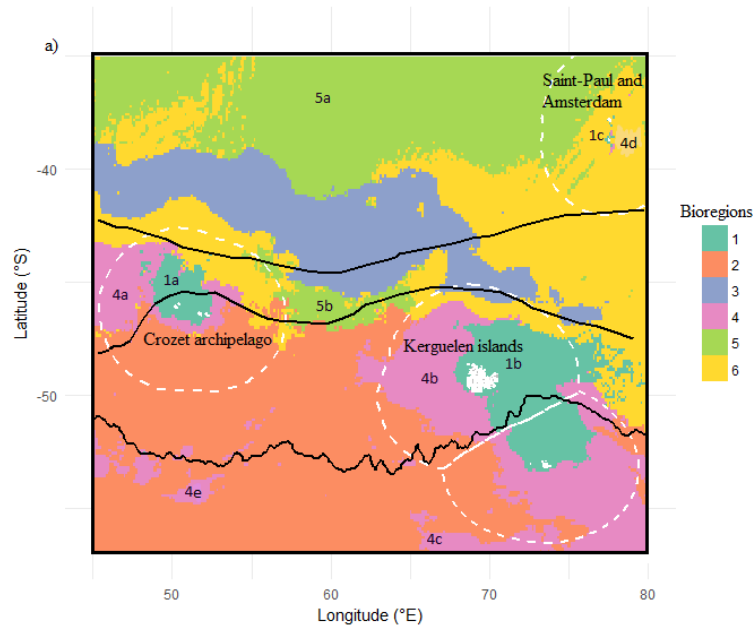
263 The first two axes of the PCA on environmental variables explained 70% of the total variance
264 (Fig. 2). Axis 1 permitted to discriminate sites according to KE and SST while axis 2
265 permitted to discriminate sites according to Bat and Chl-*a*. The clustering on the first two axes
266 of the PCA on environmental variables identified six distinct bioregions, a number of clusters
267 that allowed us also to describe the study area with sufficient detail to make sense from an
268 ecological point of view (Fig. 2). Indeed, Axis 1 opposes bioregions with relatively high KE
269 and SST (Bioregions 3, 5 and 6) to bioregions with lower KE and SST (Bioregions 4 and 2)
270 and axis 2 further opposes one bioregion with high Chl-*a* and Bat (Bioregion 1) to the others
271 (Fig. 2). The 6 bioregions are mapped and their environmental variability described in Fig. 3,

272 while Table 2 provides a synthetic overview of their localization and environmental
273 characteristics.

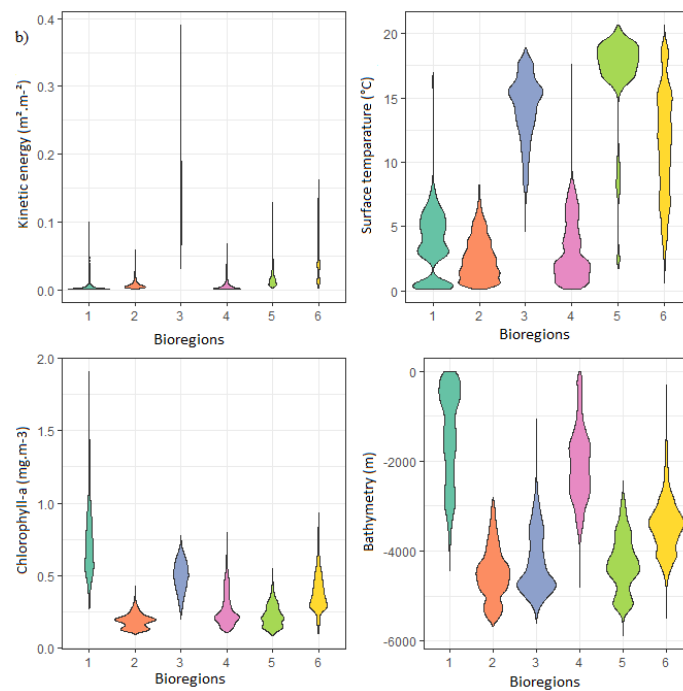


274

275 **Fig. 2.** Principal Component Analysis (PCA) of environmental parameters (SST: Sea Surface
276 Temperature ($^{\circ}\text{C}$); KE: Kinetic Energy ($\text{m}^2.\text{s}^{-2}$); Chl-*a*: concentration of Chlorophyll-*a*
277 ($\text{mg}.\text{m}^{-3}$) and Bat: Bathymetry (m)) on the two first significant axes of the PCA (Dim1,
278 Dim2)). V1= longitude and V2= latitude are supplementary variables that do not influence the
279 PCA. The colour of the 6 clusters is represented on the observations and concentration
280 ellipses.



281



282

283 **Fig. 3.** Bioregions defined by SST, KE, Chl-*a* and Bat (SST: Sea Surface Temperature; KE:
 284 Kinetic Energy; Chl-*a*: concentration of Chlorophyll-*a* and Bat: Bathymetry). Map of the six
 285 bioregions and position of the 3 main hydrological fronts (from north to south: STF, SAF and
 286 PF), the white dashed lines correspond to the exclusive economic zones (a). Violin plots of
 287 environmental parameters (SST, KE, Chl-*a* and Bat) according to the six bioregions (b).

288 **Table 2.** Descriptions of the six bioregions identified in the study area and shown in Fig. 2
 289 and Fig. 3.

Bioregions	Localization	Characteristics
1	Shelf and high productivity off-shelf waters	-Cold SST (min=0.11°C, mean=3.57°C, max=16.96°C) -Low KE(min= 0.00 m ² .s ⁻² , mean=0.00 m ² .s ⁻² , max= 0.09 m ² .s ⁻²) -High Chl- <i>a</i> (min=0.27 mg.m ⁻³ , mean= 0.73 mg.m ⁻³ , max= 1.91 mg.m ⁻³) - Shallow sea (min=-4443.0m, mean=-1434.7m, max=-2.0m)
2	Deep Eastern Part of the Enderby basin	-Cold SST (min=0.19°C, mean=2.59°C, max=8.21°C) -Low KE (min=0,00 m ² .s ⁻² , mean=0.01 m ² .s ⁻² , max=0.05 m ² .s ⁻²) -Low Chl- <i>a</i> (min=0.09 mg.m ⁻³ , mean=0.19 mg.m ⁻³ , max=0.42 mg.m ⁻³) -Deep sea (min=-5680m, mean=-4499m, max=-2801m)
3	High turbulence areas of SAF and SFT	-Hot SST (min=4.66°C, mean=14.29°C, max=18.93°C)

		<p>-High KE (min=0.03 m².s⁻², mean=0.15 m².s⁻², max=0.39 m².s⁻²)</p> <p>-Moderate Chl-<i>a</i> (min=0.20 mg.m⁻³, mean=0.50 mg.m⁻³, max=0.77 mg.m⁻³)</p> <p>-Deep sea (min=-5595m, mean=- 4271m, max=-1072m)</p> <p>This ecoregion is highly influenced by KE</p>
4	Island shelves less productive areas and seamounts	<p>-Cold SST(min=0.18°C, mean=3.16°C, max=17.62°C)</p> <p>-Low KE (min=0.00 m².s⁻², mean=0.01 m².s⁻², max=0.06 m².s⁻²)</p> <p>-Low Chll-<i>a</i> (min=0.10 mg.m⁻³, mean=0.26 mg.m⁻³, max=0.80 mg.m⁻³)</p> <p>-Shallow sea (min=-4791m, mean=- 2087m, max=-13m)</p>
5	Indian Ocean Deep	<p>-High SST (min=1.74°C, mean=17.01°C, max=20.69°C)</p> <p>-Low KE (min=0.00 m².s⁻², mean=0.02 m².s⁻², max=0.12 m².s⁻²)</p> <p>-Low Chl-<i>a</i> (min=0.08 mg.m⁻³, mean=0.22 mg.m⁻³, max=0.55</p>

		mg.m ⁻³)
		-Deep sea (min=-5887m, mean=-4283m, max=-2437m)
6	Indian ridges subtropical	-High SST (min=0.62°C, mean=7.98°C, max=20.69°C)
		-Low KE(min=0.00 m ² .s ⁻² , mean=0.05 m ² .s ⁻² , max=0.16 m ² .s ⁻²)
		-Low Chl- <i>a</i> (min=0.10 mg.m ⁻³ , mean=0.38 mg.m ⁻³ , max=0.93 mg.m ⁻³)
		-Deep sea (min=-5497m, mean=-3433m, max=-319m)

290

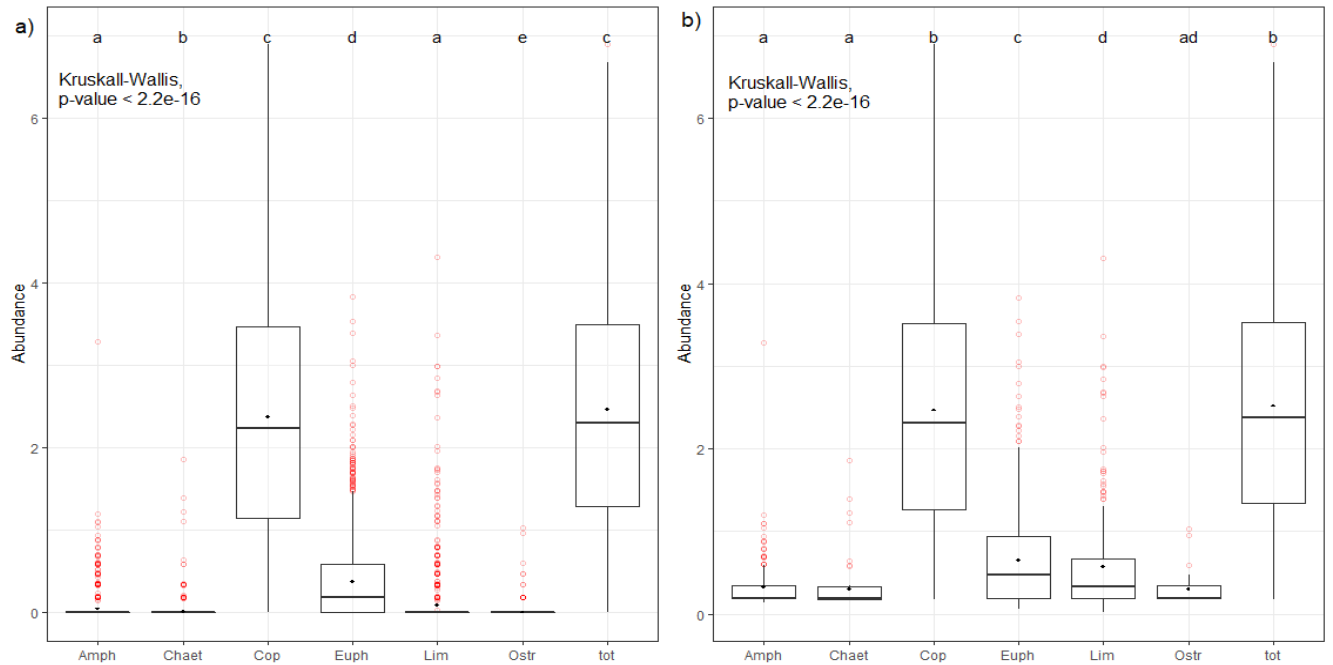
291 **3.2. Characterization of zooplankton sampling**

292 The Kruskal-Wallis test showed that the abundance of zooplankton sampled in the surface
 293 layer varied significantly between the different taxa (Fig. 4a). Specifically, we found that (i)
 294 copepods were more abundant than the other taxa, (ii) the abundance of copepods was not
 295 significantly different from the total abundance, (iii) *Limacina* and amphipod taxa present
 296 similar abundances.

297 In addition, when performing the same analyses without the zero abundance values of
 298 the different taxa, we found that the abundance of copepods, euphausiids and *Limacina*
 299 differed significantly from each other (Fig. 4b). As the abundance of euphausiids and
 300 *Limacina* was significantly higher than the abundance of ostracods, chaetognaths and

301 amphipods (Fig. 4b) and represent the vast majority of the zooplankton sampled, we decided
302 to focus the following statistical analyses only on copepods, euphausiids and *Limacina*.

303



304

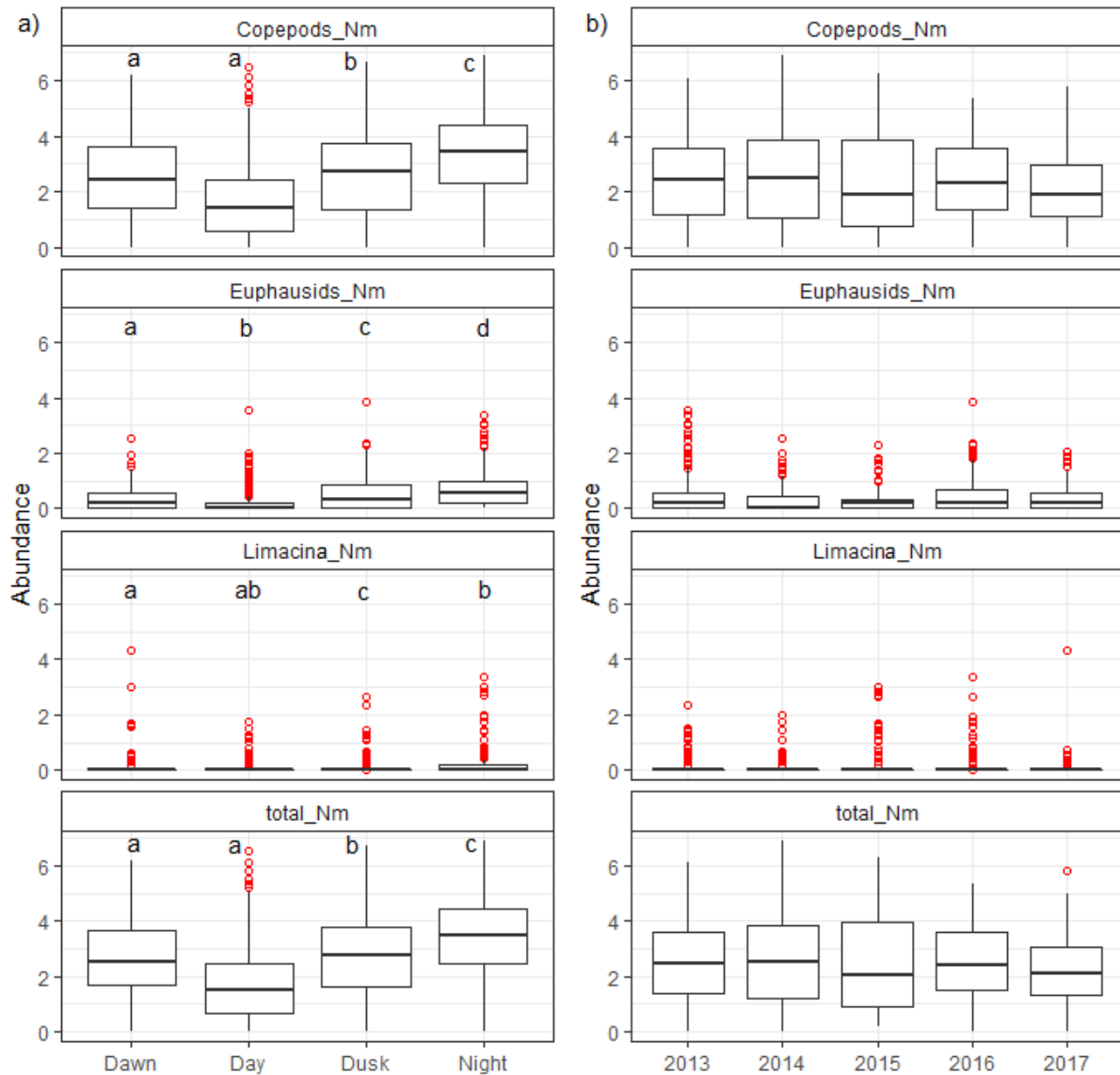
305 **Fig. 4.** Distribution of values of abundance by taxon (number of individuals per nautical mile)
306 (Amph = Amphipods, Chaet= Chaetognaths, Cop = Copepods, Euph= Euphausiids, Lim =
307 *Limacina*, Ostr= Ostracods, tot= total zooplankton abundance). On the left the abundance
308 values are transformed into $\log(x+1)$ (a) and on the right the abundance values are
309 transformed into $\log(x+1)$ and without the zero values (b). The outliers are in red. Following
310 the Wilcoxon post-hoc tests, the letters (a, b, c, d, e) correspond to the representation of
311 significance. If two taxa share the same letter then they are not significantly different, and on
312 the contrary, if two taxa do not share the same letter, then they are significantly different.

313 3.3. Temporal variations in zooplankton abundance

314 Kruskal-Wallis analyses and the post-hoc tests of Wilcoxon generally showed that the
315 abundance of zooplankton sampled in the surface layer was significantly higher at night and
316 lower during the day (Fig. 5a). Kruskal-Wallis analyses showed that the abundance of

317 zooplankton sampled in the surface layer did not vary significantly from year to year (Fig.
318 5b).

319



320

321 **Fig. 5.** Distribution of abundance value of copepods, euphausiids, *Limacina* and total
322 abundance of zooplankton transformed into a log (x+1) (number of individuals per nautical
323 mile (Nm)) according to different periods of the day (a). Distribution of abundance values of
324 copepods, euphausiids, *Limacina* and total abundance of zooplankton transformed into a log
325 (x+1) (number of individuals per nautical mile,) according to different years (b). The outliers
326 are in red. Following the Wilcoxon post-hoc tests, the letters (a, b, c, d, e) correspond to the

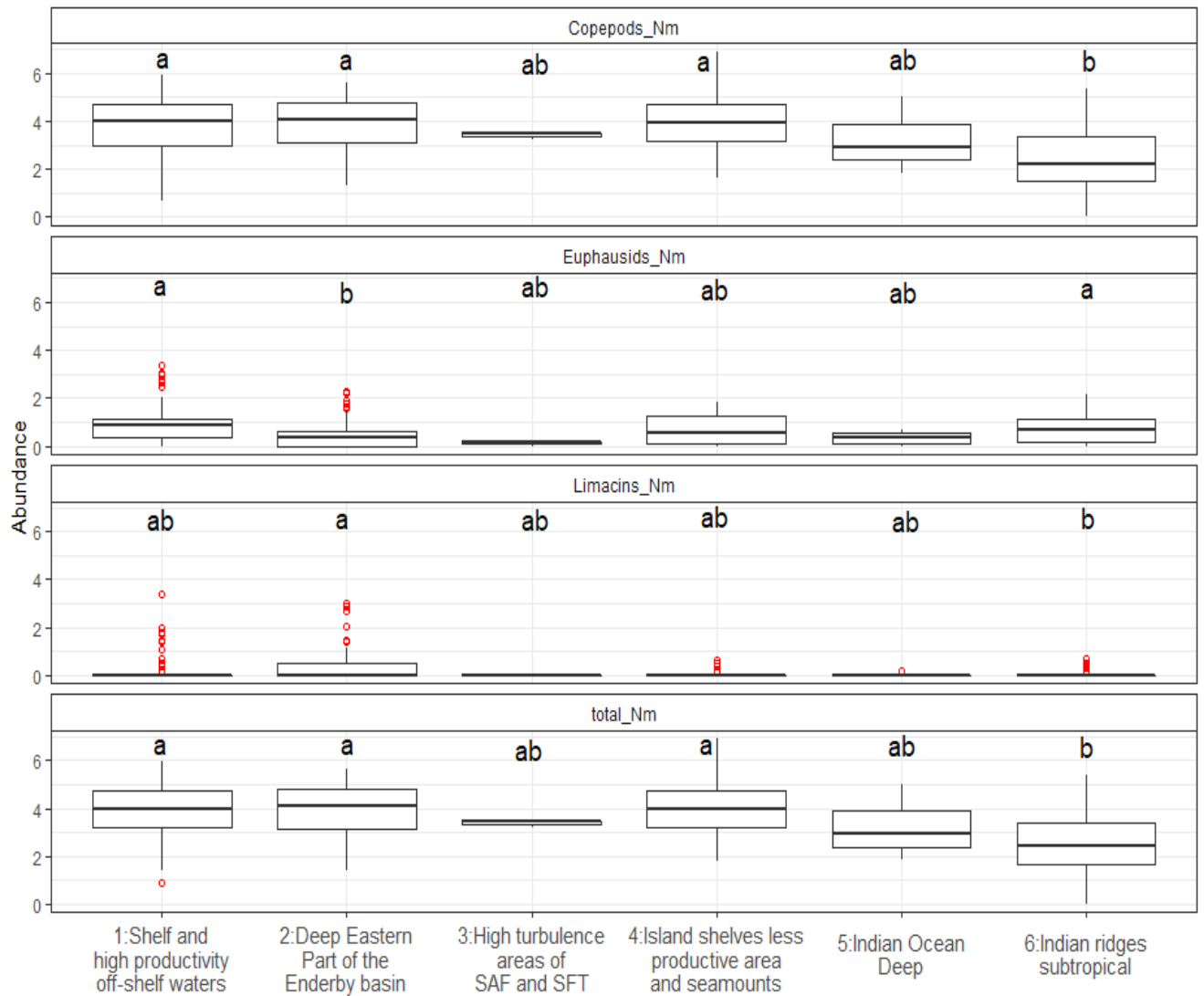
327 representation of significance. If two periods of the day share the same letter, then they are
328 not significantly different, and, on the contrary, if two periods of the day do not share the
329 same letter, then they are significantly different.

330 **3.4. Variations in zooplankton abundances across bioregions**

331 The copepod, *Limacina* and total night abundances did not differ significantly between
332 Bioregions 1 to 5 (Fig. 6). Nonetheless, copepod, *Limacina* and total night abundances were
333 the lowest in Bioregion 6, with significant differences with Bioregions 1, 2, and 4 depending
334 on the group (Fig. 6). Euphausiid abundance did not differ significantly among Bioregions 1
335 and 3 to 6, but was significantly lower in Bioregion 2 than in Bioregions 1 and 6 (Fig. 6).

336 The bioregions identified in the cluster analysis are differently represented by the
337 zooplankton samples. In particular, Bioregion 3 and Bioregion 5 are largely under-sampled
338 with respectively 3 and 11 samples collected within the five campaigns. This may explain
339 why the zooplankton abundance found there did not differ significantly from any bioregion
340 (Fig. 6).

341



342
343

344 **Fig. 6.** Distribution of values of night abundances of copepods, euphausiids and *Limacina*
 345 transformed into a log (x+1) (number of individuals per nautical mile (Nm)) according to the
 346 different bioregions (the sample sizes for each Bioregion: Bioregion 1: 77 samples; Bioregion
 347 2: 84 samples; Bioregion 3: 3 samples; Bioregion 4: 43 samples; Bioregion 5: 11 samples;
 348 Bioregion 6: 120 samples). Following the Wilcoxon post-hoc tests, the letters (a, b, c, d, e)
 349 correspond to the representation of significance. If two bioregions share the same letter then
 350 they are not significantly different, and, on the contrary, if two bioregions do not share the
 351 same letter, then they are significantly different.

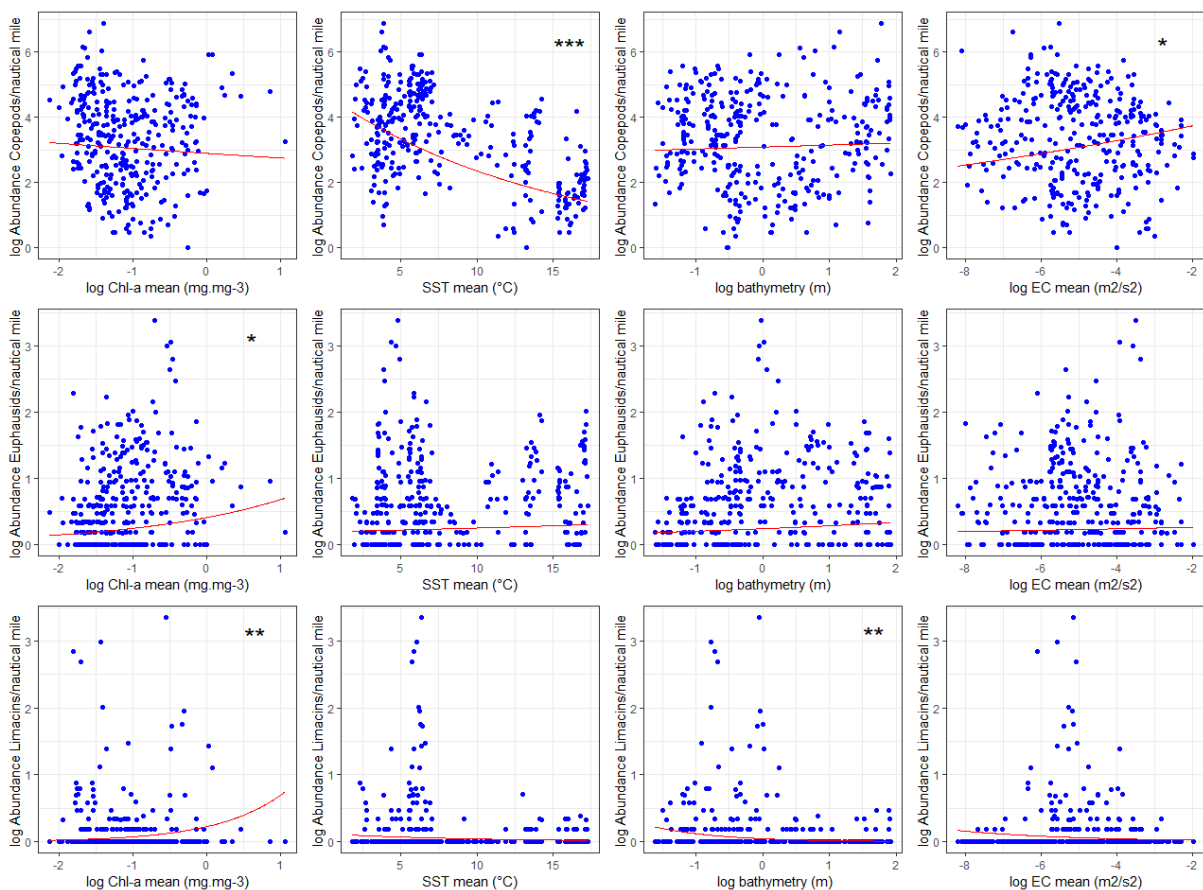
352 **3.5. Variations in zooplankton abundance with environmental parameters**

353 The first GLM model showed that the night abundance of copepods was significantly related
 354 to mean SST and KE. Specifically, the abundance of copepods decreased as the mean SST
 355 increase, whereas it slightly increased as the mean KE increased (Fig. 7).

356 The second GLM model showed that the night abundance of euphausiids was
 357 significantly related to the mean Chl-*a* concentration. Specifically, the abundance of
 358 euphausiids increased as the mean Chl-*a* increased (Fig. 7).

359 The third GLM model showed that the night abundance of *Limacina* was significantly
 360 related to mean Chl-*a* and Bat. Specifically, the abundance of *Limacina* increased as the mean
 361 Chl-*a* increased and decreased as the mean Bat increased (Fig. 7).

362



363

364 **Fig. 7.** Log(x+1) of night abundances of the different taxa (TOP: copepods, MIDDLE :
 365 euphausiids, BOTTOM: *Limacina*, all represented as the number of individuals per nautical

366 mile) as a function of the log of Chl-*a*: chlorophyll-*a* concentration ($\text{mg}\cdot\text{m}^{-3}$), SST: sea
367 surface temperature ($^{\circ}\text{C}$), Bat: bathymetry (m) and the log of KE: kinetic energy ($\text{m}^2\cdot\text{s}^{-2}$). * =
368 $p < 0.05$, ** = $p < 0.01$, *** = $p < 0.001$ (GLM).

369

370 **4. DISCUSSION**

371 In this study, we provided a new set of epipelagic bioregions for the South Indian Ocean and
372 the Indian part of the Southern Ocean at macro- and meso-scale according to their
373 environmental characteristics. Furthermore, we highlighted how the abundance of the
374 different zooplankton taxa varied spatially with environmental conditions.

375 **4.1. Bioregionalization of the Indian part of the Southern Ocean and adjacent South** 376 **Indian Ocean**

377 The six bioregions were determined according to three physical environmental parameters
378 (sea surface temperature, kinetic energy, bathymetry) and chlorophyll-*a* concentration which
379 is considered as a proxy of the surface primary production. These bioregions provide a
380 synthetic and integrated overview of contrasting environments characterized by different
381 biophysical processes (Table 2). In accordance with previous studies by Grant et al. (2006)
382 and Raymond (2014), the six bioregions we identified follow a latitudinal pattern. However,
383 our study included the Southern part of the Indian Ocean (Bioregions 3, 5 and 6 and the
384 islands of Saint Paul and Amsterdam) in addition to the Southern Ocean (Bioregions 1, 2 and
385 4). Therefore, this study provides details about the transition between these two oceans which
386 are separated by different major fronts, mainly the Sub-Antarctic and the Subtropical Fronts.
387 The main characteristics of the six bioregions are described below.

388 Bioregion 1 is mainly located to the east of the Kerguelen Plateau and north of the
389 Heard Plateau, on the central and northern part of the Crozet Plateau and in a small extent,
390 around the St. Paul Islands and the New Amsterdam Plateau. This region corresponds to areas
391 with high chlorophyll-*a* concentrations (Fig. 3). Indeed, the distribution of chlorophyll-*a* in
392 the Southern Ocean is dominated by a number of recurrent blooms observed downstream of
393 islands (Sokolov & Rintoul, 2007). These blooms are sustained by the iron enrichment of
394 water masses from the Sub-Antarctic Islands and their plateaus (Blain et al., 2001; Sanial et
395 al., 2014; Graham et al., 2015; d'Ovidio et al., 2015).

396 Bioregion 2 is located in the deep eastern part of the Enderby Basin in the Southern
397 Ocean, south of SAF. The kinetic energy is low, as well as the sea surface temperature and
398 chlorophyll-*a* concentration, thus representing a typical HNLC zone. South of Crozet, the PF
399 at about 50° S has a low current velocity (Park et al., 1993; Pollard and Read, 2001; Pollard et
400 al., 2002; Pollard et al., 2007). The low chlorophyll-*a* concentrations are a consequence of
401 iron deficiency (Boyd et al., 2000; Boyd et al., 2007; Pollard et al., 2007; De Baar et al.,
402 2005). Indeed, this area is very deep and remote from islands, shallow plateaus or seamounts
403 (which are the main source of iron in the region) (e.g. Ardyna et al., 2017).

404 Bioregion 3 corresponds to the physically-energetic areas of the Indian Ocean
405 characterized by high kinetic energy (Fig. 3). The ACC flows mainly to the north of the
406 Crozet and Kerguelen plateau, the latter being a major obstacle to the eastward flow of the
407 ACC (Roquet et al., 2009). High kinetic energies in this region indicate intense horizontal
408 velocities generated by the ACC and the Agulhas Current. After Bioregion 1, Bioregion 3 is
409 the area with the higher chlorophyll-*a* concentration. Indeed, the intense horizontal velocities
410 allow the transport of nutrient from the shallow topographies around the African coasts into
411 the open ocean for thousands of kilometers sustaining the phytoplankton productivity (e.g.
412 Ardyna et al. 2017). In addition, this area is characterized by an intense mesoscale activity
413 associate to meanders, eddies, filaments and fronts which may also enhance the primary

414 production (e.g. Flierl and Davies, 1993; Oschlies and Graçon, 1998; Machu and Garçon,
415 2001; Lévy, 2008).

416 Bioregion 4 is characterized by shallow to mid bathymetry and low chlorophyll-*a*
417 concentrations and is located either in the deepest parts of the island shelves, mainly in the
418 western part of these shelves, and over complex seamounts (Figs. 2 and 3). The relative low
419 chlorophyll-*a* concentration in the western part of the shelf areas (Fig. 3b) may be explained
420 by the zonal location of this bioregion relatively to the plateau. Indeed, due to the main
421 eastward circulation of the ACC, the iron enrichment of the water masses is more intense in
422 the eastern part of the shelves and offshore, generating a longitudinal chlorophyll-*a* gradient
423 upstream and downstream of the plateau (e.g Sanial et al., 2014; d'Ovidio et al., 2015). This
424 difference can be observed with contrasted chlorophyll-*a* concentrations between Bioregion 4
425 (western flank, lower chlorophyll-*a* concentration) and Bioregion 1 (eastern flank, higher
426 chlorophyll-*a* concentration). The relative shallow depth of the areas of the Bioregion 4 which
427 are located offshore from the islands is explained by the numerous seamounts included in
428 these areas. These are the large Skif bank to the south-west of Kerguelen and the Elan Bank
429 south-west of Heard at the limit of the study area (Bioregion 4b in Fig. 3). South of Crozet,
430 different seamounts of smaller size such as Ob, Lena and Marion Dufresne are located near
431 the PF (Bioregion 4e in Fig. 3). The presence of shallow seamounts may also stimulate the
432 nutrient input in the euphotic layer thus sustaining higher chlorophyll-*a* concentrations
433 compared to the surrounding water of the abyssal plain (Bioregion 2) (e.g. Pitcher et al.,
434 2008).

435 Bioregion 5 is located in the Subtropical Indian Ocean (5a) and to the north of the STF
436 (5b), two areas of abyssal plains or hills (Harris et al., 2014). They are characterized by higher
437 temperatures and represent the deepest zones of the Indian Ocean. Bioregion 5a is the
438 warmest region and Bioregion 5b is the deepest region (Fig. 3) (Harris et al., 2014). The low

439 chlorophyll-*a* concentrations found in Bioregion 5 are typical of the hyperoligotrophic waters
440 of the subtropical gyres (e.g. McClain et al., 2004; Morel et al., 2010).

441 Bioregion 6 is characterized by a large thermal amplitude and can be considered as an
442 Indian Subtropical region with deep bathymetry and low kinetic energy. This area also
443 includes shallower seamounts at the mid-ocean ridges (Harris et al., 2014). This area is
444 divided into two sub-areas by Bioregion 3. However, the main part is located to the northeast
445 of the study area, around the St Paul and Amsterdam Islands, and includes part of the
446 Southeast Indian Ridge. The northwestern part includes part of the Southwest Indian Ridge in
447 Indian Ocean.

448 **4.2. Spatial variations in zooplankton abundance**

449 Consistent with previous CPR studies conducted in various regions of the Southern
450 Ocean, we found that copepods account for most of the zooplankton biomass (Hunt and
451 Hosie, 2003; Hunt and Hosie, 2006a; Hunt and Hosie, 2006b; Hosie et al., 2003; Takahashi et
452 al., 2002; Takahashi et al., 2010; Takahashi et al., 2011). Our analyses of copepods,
453 euphausids and *Limacina* sampled at night permitted to reveal the spatial patterns in the
454 abundance of the different taxa across our study area encompassing the Southern Ocean and
455 the South Indian Ocean. These spatial patterns are explained by (i) the high dependence of
456 copepod abundance on sea surface temperature and, to a lesser extent, kinetic energy; (ii) the
457 high dependence of euphausid abundance on chlorophyll-*a* concentration; (iii) the high
458 dependence of *Limacina* abundance on chlorophyll-*a* concentration and shallow bathymetry.

459 The GLM models indicate that the copepods were most abundant in the cold waters of
460 the Southern Ocean. Accordingly, the abundance of copepods was significantly highest in
461 Bioregions 1, 2 and 4, which are located in the southern part of the study area and correspond
462 to the coldest zones in the Permanent Open Ocean Zones, than in Bioregion 6. This is because
463 temperature has major effects on the physiology of zooplankton in Antarctic and is therefore

464 one of the main factors defining its biogeographic distributions (Pörtner et al., 2007).
465 Furthermore, the GLM models revealed a greater abundance of copepods in physically-
466 energetic waters. Although copepods are quite abundant in Bioregion 3, i.e. the most
467 physically-energetic zone of our study area located in the Subtropical and Sub-Antarctic
468 regions, their abundance in this under-sampled bioregion does not differ significantly from the
469 others. Further *in situ* analysis of zooplankton abundance in this high turbulent region could
470 allow us testing this relationship within pelagic bioregions.

471 The GLM models also revealed that euphausiids were more abundant in chlorophyll-*a*
472 rich areas. Specifically, they were significantly less abundant in low productive open ocean
473 waters of Bioregion 2 compared to the shelf and off-shelf high productivity areas of Bioregion
474 1. The higher abundance of euphausiids in the Indian ridges subtropical waters of Bioregion 6
475 could also be related to the higher chlorophyll-*a* found there. This positive relationship
476 between the abundance of euphausiids and chlorophyll-*a* is not surprising because primary
477 production corresponds to phytoplankton, the main food of zooplankton. This further supports
478 previous studies showing that zooplankton biomass is globally found to be positively related
479 to the phytoplankton biomass (Irigoiien et al., 2004).

480 The GLM models also identify a positive relationship between *Limacina* abundance
481 and chlorophyll-*a*, and a positive relationship of *Limacina* abundance with bathymetry.
482 Consequently, the higher abundance of *Limacina* in Bioregion 2 could be related to the more
483 important depths found there. Although not significantly, the shallow shelves of Bioregion 1
484 also display lower *Limacina* abundance. Further investigations should be done in order to
485 confirm the relationship between *Limacina* abundance and shallow topographies, poorly
486 covered by the existing literature.

487 Overall, although there are correlations between the three groups of zooplankton and
488 environmental conditions, the different zooplankton groups do not map very well onto the
489 bioregions. Several causes could explain this. Firstly, some key transition bioregions essential

490 for understanding the variability of the studied region - such as Bioregion 3, the high turbulent
491 area between the SAF and the STF - have been under-sampled. Secondly, the coarse
492 taxonomic resolution used in this study could have hampered the identification of clear
493 differences between bioregions. As suggested by previous studies, and given the large
494 temperature gradient sampled, species level data would likely better reveal differences
495 between bioregions in our study area (e.g. Hunt et al., 2011).

496 **4.3. Limits and perspectives**

497 The environmental parameters used in this study come from satellite observations averaged
498 over time and space. Due to their large spatial coverage, these data can be used to distinguish
499 spatial environmental variations between areas in two dimensions (latitude and longitude) and
500 to explain surface variation in zooplankton abundance. However, these measurements do not
501 take into account how environmental conditions and zooplankton abundance vary according
502 to the vertical dimension, i.e. the depth of the zone. The environmental properties of the water
503 column can influence the ecology of many species along the trophic webs, including top
504 predators (Bost et al., 2009). In addition, we did not consider all the environmental parameters
505 that can affect the abundance of zooplankton. Future studies may consider delineating
506 bioregions in three dimensions and integrating other potentially harmful environmental
507 parameters for zooplankton (e.g. ocean acidification, UV or nutrient levels) to better
508 anticipate the impact of environmental changes on zooplankton in each bioregion.

509 **4.4. Conclusion**

510 In this study, we first characterized bioregions based on physical parameters and chlorophyll-
511 *a*. We then investigated the variations in zooplankton abundance across these bioregions in
512 order to move from a bioregionalization procedure towards an ecoregionalization procedure
513 by progressively integrating species assemblages. Initially, the temporal variations in surface

514 abundance are explained by nocturnal migrations, i.e. zooplankton is more abundant at night
515 in the surface layer. The variations in zooplankton abundance are also explained spatially by
516 environmental parameters and, to a lesser degree, by the bioregions. Future campaigns in the
517 under-sampled transition bioregions are needed to determine whether the observed variations
518 could be explained more consistently by the bioregionalization at the meso- and macro-scale,
519 or whether other spatial scales should be considered for their representation.

520 This study complements previous ecoregionalization work (Koubbi et al., 2016a;
521 2016b) carried out at smaller spatial scales in the ocean zone around Kerguelen and/or Crozet
522 on the pelagic realm, including seabirds and marine mammals. This work is therefore a
523 further step towards the identification of coherent ecoregions. Once constructed and
524 characterized, these ecoregions will serve as a basis for optimizing marine biodiversity
525 conservation strategies in this part of the Southern Ocean where marine reserves around
526 Crozet, Kerguelen and St-Paul / New Amsterdam were declared by France in 2016 (Koubbi
527 et al., 2016a; 2016b).

528 An important step forward in ecoregionalization would be the integration of all species
529 in the food web - from phytoplankton to zooplankton, fish and top predators. Indeed, as the
530 different trophic groups do not respond in the same way to spatiotemporal variations in their
531 environment (Koubbi et al., 2011), the way forward to an ecoregionalization of this area is to
532 identify indicator or assemblages from distinct trophic levels. Future work should therefore
533 investigate further regionalization of less studied mesopelagic fish. Then, it would be
534 interesting to integrate the regionalizations of the different trophic levels in order to obtain a
535 comprehensive regionalization.

536 **Acknowledgements**

537 This work was supported by IPEV, the Flotte Océanographique Française, Zone Atelier
538 Antarctique - CNRS, the European H2020 International Cooperation project MESOPP [grant
539 number 692173] and the TAAF (Southern Lands and Antarctic French Territories) natural
540 reserve. It is related to the SCAR Southern Ocean CPR programme and the Global Alliance
541 CPR Surveys We thank the IPEV teams who were in charge of logistics during the
542 oceanographic surveys, as well as the crew members of the R/V “Marion Dufresne”. We
543 warmly thank Chloé Mignard and Baptiste Sérandour for participating in processing and
544 identification of samples, and Patrice Pruvost for taking in charge the zooplankton sampling
545 during the 2016 survey.

546 **References**

- 547 Ainley, D. G., Ballard, G., & Weller, J. (2010). Ross Sea bioregionalization, part I: validation
548 of the 2007 CCAMLR bioregionalization workshop results towards including the Ross
549 Sea in a representative network of marine protected areas in the Southern Ocean.
550 *CCAMLR reference number: CCAMLR WG-EMM-10/11.*
- 551 Ardyna, M., Claustre, H., Sallée, J. B., D'Ovidio, F., Gentili, B., Van Dijken, G., ... Arrigo, K.
552 R. (2017). Delineating environmental control of phytoplankton biomass and phenology
553 in the Southern Ocean. *Geophysical Research Letters*, 44(10), 5016-5024.
554 <https://doi.org/10.1002/2016GL072428>
- 555 Batten, S. D., Abu-Alhaija, R., Chiba, S., Edwards, M., Graham, G., Jiyothibabu, R., ... Ostle,
556 C. (2019). A global plankton diversity monitoring program. *Frontiers in Marine Science*,
557 6, 321.
- 558 Béhagle, N., Cotté, C., & Ryan, T. E. (2016). Acoustic micronektonic distribution is
559 structured by macroscale oceanographic processes across 20-50°S latitudes in the South-
560 Western Indian Ocean. *Deep-Sea Research Part I: Oceanographic Research Papers*,
561 110, 20–32. <https://doi.org/10.1016/j.dsr.2015.12.007>
- 562 Biavati, G. (2014). *RAtmosphere: Standard Atmospheric profiles*. Retrieved from
563 <https://cran.r-project.org/package=RAtmosphere>
- 564 Blain, S., Tréguer, P., Belviso, S., Bucciarelli, E., Denis, M., Desabre, S., ... Razouls, S.
565 (2001). A biogeochemical study of the island mass effect in the context of the iron
566 hypothesis: Kerguelen Islands, Southern Ocean. *Deep Sea Research Part I:
567 Oceanographic Research Papers*, 48(1), 163–187. [https://doi.org/10.1016/S0967-
568 0637\(00\)00047-9](https://doi.org/10.1016/S0967-0637(00)00047-9)

569 Blain, S., Quéguiner, B., Armand, L., Belviso, S., Bombled, B., Bopp, L., ... Wagener, T.
570 (2007). Effect of natural iron fertilization on carbon sequestration in the Southern Ocean.
571 *Nature*, 446(7139), 1070–1074. <https://doi.org/10.1038/nature05700>

572 Bost, C. A., Cotté, C., Bailleul, F., Cherel, Y., Charrassin, J. B., Guinet, C., ... Weimerskirch,
573 H. (2009). The importance of oceanographic fronts to marine birds and mammals of the
574 southern oceans. *Journal of Marine Systems*, 78(3), 363–376.
575 <https://doi.org/10.1016/j.jmarsys.2008.11.022>

576 Boyd, P. W., Watson, A. J., Law, C. S., Abraham, E. R., Trull, T., Murdoch, R., ... Zeldis, J.
577 (2000). A mesoscale phytoplankton bloom in the polar Southern Ocean stimulated by
578 iron fertilization. *Nature*, 407(6805), 695–702. <https://doi.org/10.1038/35037500>

579 Boyd, P. W., Jickells, T., Law, C. S., Blain, S., Boyle, E. A., Buesseler, K. O., ... Watson, A.
580 J. (2007). Mesoscale Iron Enrichment Experiments 1993-2005: Synthesis and Future
581 Directions. *Science*, 315(5812), 612–617. <https://doi.org/10.1126/science.1131669>

582 Boyd, P. W., & Ellwood, M. J. (2010). The biogeochemical cycle of iron in the ocean. *Nature*
583 *Geoscience*, 3(10), 675. <https://doi.org/10.1038/ngeo964>

584 Broad, W. J. (1998). *The Universe Below: Discovering the Secrets of the Deep Sea*. Simon
585 and Schuster, New-York, USA.

586 Calinsky, T., & Harabasz, J. (1974). A dendrite method for cluster analysis. *Communications*
587 *in Statistics-Theory and Methods*, 3(1), 1–27. Retrieved from www.bogucki.com.pl,

588 Constable, A. J., Melbourne-Thomas, J., Corney, S. P., Arrigo, K. R., Barbraud, C., Barnes,
589 D. K. A., ... Ziegler, P. (2014). Climate change and Southern Ocean ecosystems I: How
590 changes in physical habitats directly affect marine biota. *Global Change Biology*, 20(10),
591 3004–3025. <https://doi.org/10.1111/gcb.12623>

592 Cotté, C., Park, Y. H., Guinet, C., & Bost, C. A. (2007). Movements of foraging king
593 penguins through marine mesoscale eddies. *Proceedings of the Royal Society B:*
594 *Biological Sciences*, 274(1624), 2385–2391. <https://doi.org/10.1098/rspb.2007.0775>

595 De Baar, H. J., De Jong, J. T., Bakker, D. C., Löscher, B. M., Veth, C., Bathmann, U., &
596 Smetacek, V. (1995). Importance of iron for plankton blooms and carbon dioxide
597 drawdown in the Southern Ocean. *Nature*, 373(6513), 412.
598 <https://doi.org/10.1038/373412a0>

599 De Baar, H. J. W., Boyd, P. W., Coale, K. H., Landry, M. R., Tsuda, A., Assmy, P., ... Wong,
600 C. S. (2005). Synthesis of iron fertilization experiments: From the iron age in the age of
601 enlightenment. *Journal of Geophysical Research C: Oceans*, 110(9), 1–24.
602 <https://doi.org/10.1029/2004JC002601>

603 De Monte, S., Cotté, C., D'Ovidio, F., Lévy, M., Le Corre, M., & Weimerskirch, H. (2012).
604 Frigatebird behaviour at the ocean-atmosphere interface: Integrating animal behaviour
605 with multi-satellite data. *Journal of the Royal Society Interface*, 9(77), 3351–3358.
606 <https://doi.org/10.1098/rsif.2012.0509>

607 D'Ovidio, F., Della Penna, A., Trull, T. W., Nencioli, F., Pujol, M. I., Rio, M. H., ... Blain, S.
608 (2015). The biogeochemical structuring role of horizontal stirring: Lagrangian
609 perspectives on iron delivery downstream of the Kerguelen Plateau. *Biogeosciences*,
610 12(19), 5567–5581. <https://doi.org/10.5194/bg-12-5567-2015>

611 Duhamel, G., Hulley, P. A., Causse, R., Koubbi, P., Vacchi, M., Pruvost, P., ... Dettai, A.
612 (2014). Biogeographic patterns of fish. In *Biogeographic Atlas of the Southern Ocean*,
613 418–421.

- 614 Flierl, G. R., & Davis, C. S. (1993). Biological effects of Gulf Stream meandering. *Journal of*
615 *Marine Research*, 51(3), 529-560. <https://doi.org/10.1357/0022240933224016>
- 616 Foster, S. D., Hill, N. A., & Lyons, M. (2017). Ecological grouping of survey sites when
617 sampling artefacts are present. *Journal of the Royal Statistical Society: Series C (Applied*
618 *Statistics)*, 66(5), 1031–1047. <https://doi.org/10.1111/rssc.12211>
- 619 Gandhi, N., Ramesh, R., Laskar, A. H., Sheshshayee, M. S., Shetye, S., Anilkumar, N., ...
620 Mohan, R. (2012). Zonal variability in primary production and nitrogen uptake rates in
621 the southwestern Indian Ocean and the Southern Ocean. *Deep-Sea Research Part I:*
622 *Oceanographic Research Papers*, 67, 32–43. <https://doi.org/10.1016/j.dsr.2012.05.003>
- 623 Graham, R. M., De Boer, A. M., van Sebille, E., Kohfeld, K. E., & Schlosser, C. (2015).
624 Inferring source regions and supply mechanisms of iron in the Southern Ocean from
625 satellite chlorophyll data. *Deep-Sea Research Part I: Oceanographic Research Papers*,
626 *104*, 9–25. <https://doi.org/10.1016/j.dsr.2015.05.007>
- 627 Grant, S., Constable, A., Raymond, B., & Doust, S. (2006). *Bioregionalisation of the*
628 *Southern Ocean*. Hobart.
- 629 Gutt, J., Bertler, N., Bracegirdle, T. J., Buschmann, A., Comiso, J., Hosie, G., ... Xavier, J. C.
630 (2015). The Southern Ocean ecosystem under multiple climate change stresses - an
631 integrated circumpolar assessment. *Global Change Biology*, 21(4), 1434–1453.
632 <https://doi.org/10.1111/gcb.12794>
- 633 Handegard, N. O., Buisson, L. Du, Brehmer, P., Chalmers, S. J., De Robertis, A., Huse, G., ...
634 Godø, O. R. (2013). Towards an acoustic-based coupled observation and modelling
635 system for monitoring and predicting ecosystem dynamics of the open ocean. *Fish and*
636 *Fisheries*, 14(4), 605–615. <https://doi.org/10.1111/j.1467-2979.2012.00480.x>

- 637 Harris, P. T., Macmillan-Lawler, M., Rupp, J., & Baker, E. K. (2014). Geomorphology of the
638 oceans. *Marine Geology*, 352, 4–24. <https://doi.org/10.1016/j.margeo.2014.01.011>
- 639 Hill, N. A., Foster, S. D., Duhamel, G., Welsford, D., Koubbi, P., & Johnson, C. R. (2017).
640 Model-based mapping of assemblages for ecology and conservation management: A case
641 study of demersal fish on the Kerguelen Plateau. *Diversity and Distributions*, 23(10),
642 1216–1230. <https://doi.org/10.1111/ddi.12613>
- 643 Hogg, O. T., Huvenne, V. A. I., Griffiths, H. J., & Linse, K. (2018). On the ecological
644 relevance of landscape mapping and its application in the spatial planning of very large
645 marine protected areas. *Science of The Total Environment*, 626, 384–398.
646 <https://doi.org/10.1016/j.scitotenv.2018.01.009>
- 647 Holm, S. (1979). Une simple procédure de test multiple à rejet séquentiel. *Journal scandinave*
648 *de statistiques*, 6, 65–70. <http://www.jstor.org/stable/4615733>
- 649 Hosie, G. ., Fukuchi, M., & Kawaguchi, S. (2003). Development of the Southern Ocean
650 Continuous Plankton Recorder survey. *Progress in Oceanography*, 58(2–4), 263–283.
651 <https://doi.org/10.1016/j.pocean.2003.08.007>
- 652 Hosie, G., Mormède, S., Kitchener, J., Takahashi, K., & Raymond, B. (2014). 10.3.Near-
653 surface zooplankton communities. In *Biogeographic Atlas of the Southern Ocean* (pp.
654 422–430).
- 655 Hunt, B. P., & Hosie, G. W. (2003). The Continuous Plankton Recorder in the Southern
656 Ocean: a comparative analysis of zooplankton communities sampled by the CPR and
657 vertical net hauls along 140 E. *Journal of Plankton Research*, 25(12), 1561–1579.
658 <https://doi.org/10.1093/plankt/fbg108>

659 Hunt, B. P. V., & Hosie, G. W. (2006). The seasonal succession of zooplankton in the
660 Southern Ocean south of Australia, part I: The seasonal ice zone. *Deep Sea Research*
661 *Part I: Oceanographic Research Papers*, 53(7), 1182–1202.
662 <https://doi.org/10.1016/j.dsr.2006.05.001>

663 Hunt, B. P. V., & Hosie, G. W. (2006). The seasonal succession of zooplankton in the
664 Southern Ocean south of Australia, part II: The Sub-Antarctic to Polar Frontal Zones.
665 *Deep Sea Research Part I: Oceanographic Research Papers*, 53(7), 1203–1223.
666 <https://doi.org/10.1016/j.dsr.2006.05.002>

667 Hunt, B.P.V., Pakhomov, E.A., Williams, R. (2011). Comparative analysis of 1980's and 2004
668 macrozooplankton composition and distribution in the vicinity of Kerguelen and Heard
669 Islands: seasonal cycles and oceanographic forcing of long-term change. *Cybiurn*, 35, 79-
670 92. <https://doi.org/10.26028/cybiurn/2011-35SP-008>

671 Irigoien, X., Huisman, J., & Harris, R. P. (2004). Global biodiversity patterns of marine
672 phytoplankton and zooplankton. *Nature*, 429(6994), 863-867.

673 IPCC, 2019. IPCC Special Report on the Ocean and Cryosphere in a Changing Climate. H.-O.
674 Pörtner, D.C. Roberts, V. Masson-Delmotte, P. Zhai, M. Tignor, E. Poloczanska, K.
675 Mintenbeck, A. Alegría, M. Nicolai, A. Okem, J. Petzold, B. Rama, N.M. Weyer (eds.).
676 In press.

677 Koubbi, P. (1993). Influence of the frontal zones on ichthyoplankton and mesopelagic fish
678 assemblages in the Crozet Basin (Indian sector of the Southern Ocean). *Polar Biology*,
679 13(8), 557–564. <https://doi.org/10.1007/BF00236398>

680 Koubbi, P., Ozouf-Costaz, C., Goarant, A., Moteki, M., Hulley, P.-A., Causse, R., ... Hosie,
681 G. (2010). Estimating the biodiversity of the East Antarctic shelf and oceanic zone for

682 ecoregionalisation: Example of the ichthyofauna of the CEAMARC (Collaborative East
683 Antarctic Marine Census) CAML surveys. *Polar Science*, 4(2), 115–133.
684 <https://doi.org/10.1016/j.polar.2010.04.012>

685 Koubbi, P., Moteki, M., Duhamel, G., Goarant, A., Hulley, P. A., O’Driscoll, R., ... Hosie, G.
686 (2011). Ecoregionalization of myctophid fish in the Indian sector of the Southern Ocean:
687 Results from generalized dissimilarity models. *Deep-Sea Research Part II: Topical*
688 *Studies in Oceanography*, 58(1–2), 170–180. <https://doi.org/10.1016/j.dsr2.2010.09.007>

689 Koubbi, P., Guinet, C., Alloncle, N., Ameziane, N., Azam, C. S., Baudena, A.,
690 ...Weimerskirch, H. (2016). Ecoregionalisation of the Kerguelen and Crozet islands
691 oceanic zone. Part I: Introduction and Kerguelen oceanic zone. *CCAMLR Document*
692 *WG-EMM-16/43*.

693 Koubbi, P., Mignard, C., Causse, R., Da Silva, O., Baudena, A., Bost, C., ... Fabri-Ruiz, S.
694 (2016). Ecoregionalisation of the Kerguelen and Crozet islands oceanic zone. Part II: The
695 Crozet oceanic zone. *CCAMLR Report*, 1-50.

696 Lê, S., Josse, J. & Husson, F. (2008). FactoMineR: An R Package for Multivariate Analysis.
697 *Journal of Statistical Software*. 25(1). pp. 1-18.

698 Legendre, P., & Legendre, L. (1998). *Numerical ecology*. Springer, New-York, USA.

699 Lehodey, P., Conchon, A., Senina, I., Domokos, R., Calmettes, B., Jouanno, J., ... Kloser, R.
700 (2015). Optimization of a micronekton model with acoustic data. *ICES Journal of*
701 *Marine Science*, 72(5), 1399-1412.

702 Lévy, M. (2008). The modulation of biological production by oceanic mesoscale turbulence.
703 In *Transport and Mixing in Geophysical Flows* (pp. 219-261). Springer, Berlin,
704 Heidelberg.

705 Longhurst, A. R. (2010). *Ecological geography of the sea*. Elsevier.

706 Machu, E., & Garçon, V. (2001). Phytoplankton seasonal distribution from SeaWiFS data in
707 the Agulhas Current system. *Journal of marine research*, 59(5), 795-812.
708 <https://doi.org/10.1357/002224001762674944>

709 Mackey, A. P., Atkinson, A., Hill, S. L., Ward, P., Cunningham, N. J., Johnston, N. M., &
710 Murphy, E. J. (2012). Antarctic macrozooplankton of the southwest Atlantic sector and
711 Bellingshausen Sea: Baseline historical distributions (Discovery Investigations, 1928–
712 1935) related to temperature and food, with projections for subsequent ocean warming.
713 *Deep Sea Research Part II: Topical Studies in Oceanography*, 59–60, 130–146.
714 <https://doi.org/10.1016/j.dsr2.2011.08.011>

715 MacQueen, J. (1967). Some methods for classification and analysis of multivariate
716 observations. *Proceedings of the Fifth Berkeley Symposium on Mathematical Statistics*
717 *and Probability*, 1(14), 281–297. <https://doi.org/10.1007/s11665-016-2173-6>

718 Martin, J. H. (1990). Glacial-interglacial CO₂ change: The iron hypothesis.
719 *Paleoceanography*, 5(1), 1-13

720 McClain, C. R., Signorini, S. R., & Christian, J. R. (2004). Subtropical gyre variability
721 observed by ocean-color satellites. *Deep Sea Research Part II: Topical Studies in*
722 *Oceanography*, 51(1-3), 281-301.

723 Meilland, J., Fabri-Ruiz, S., Koubbi, P., Monaco, C. Lo, Cotte, C., Hosie, G. W., ... Howa, H.
724 (2016). Planktonic foraminiferal biogeography in the Indian sector of the Southern
725 Ocean: Contribution from CPR data. *Deep-Sea Research Part I: Oceanographic*
726 *Research Papers*, 110, 75–89. <https://doi.org/10.1016/j.dsr.2015.12.014>

727 Morel, A., Claustre, H., & Gentili, B. (2010). The most oligotrophic subtropical zones of the
728 global ocean: similarities and differences in terms of chlorophyll and yellow substance.
729 *Biogeosciences*, 7(10), 3139-3151. <https://doi.org/10.5194/bg-7-3139-2010>

730 NG, A. (2012). *Clustering with the k-means algorithm. Machine Learning*.

731 Oschlies, A., & Garçon, V. (1998). Eddy-induced enhancement of primary production in a
732 model of the North Atlantic Ocean. *Nature*, 394(6690), 266.
733 <https://doi.org/10.1038/28373>

734 Orsi, A. H., Whitworth, T., & Nowlin, W. D. (1995). On the meridional extent and fronts of
735 the Antarctic Circumpolar Current. *Deep-Sea Research Part I*, 42(5), 641–673.
736 [https://doi.org/10.1016/0967-0637\(95\)00021-W](https://doi.org/10.1016/0967-0637(95)00021-W)

737 Park, Y. H., Gambéroni, L., & Charriaud, E. (1991). Frontal structure and transport of the
738 Antarctic Circumpolar Current in the south Indian Ocean sector, 40–80°E. *Marine*
739 *Chemistry*, 35(1–4), 45–62. [https://doi.org/10.1016/S0304-4203\(09\)90007-X](https://doi.org/10.1016/S0304-4203(09)90007-X)

740 Park, Y. H., Gamberoni, L., & Charriaud, E. (1993). Frontal structure, water masses, and
741 circulation in the Crozet Basin. *Journal of Geophysical Research*, 98(C7), 12361–12385.
742 <https://doi.org/10.1029/93jc00938>

743 Park, Y. H., Pollard, R. T., Read, J. F., & Leboucher, V. (2002). A quasi-synoptic view of the
744 frontal circulation in the Crozet Basin during the Antares-4 cruise. *Deep-Sea Research*
745 *Part II: Topical Studies in Oceanography*, 49(9–10), 1823–1842.
746 [https://doi.org/10.1016/S0967-0645\(02\)00014-0](https://doi.org/10.1016/S0967-0645(02)00014-0)

747 Park, Y. H., Roquet, F., Durand, I., & Fuda, J. L. (2008). Large-scale circulation over and
748 around the Northern Kerguelen Plateau. *Deep-Sea Research Part II: Topical Studies in*
749 *Oceanography*, 55(5–7), 566–581. <https://doi.org/10.1016/j.dsr2.2007.12.030>

- 750 Pitcher, T. J., Morato, T., Hart, P. J., Clark, M. R., Haggan, N., & Santos, R. S. (Eds.). (2008).
751 *Seamounts: ecology, fisheries and conservation*. John Wiley & Sons
- 752 Pollard, R. T., & Read, J. F. (2001). Circulation pathways and transports of the Southern
753 Ocean in the vicinity of the Southwest Indian Ridge. *Journal of Geophysical Research:*
754 *Oceans*, 106(C2), 2881–2898. <https://doi.org/10.1029/2000JC900090>
- 755 Pollard, R. T., Lucas, M. I., & Read, J. F. (2002). Physical controls on biogeochemical
756 zonation in the Southern Ocean. *Deep-Sea Research Part II: Topical Studies in*
757 *Oceanography*, 49(16), 3289–3305. [https://doi.org/10.1016/S0967-0645\(02\)00084-X](https://doi.org/10.1016/S0967-0645(02)00084-X)
- 758 Pollard, R. T., Venables, H. J., Read, J. F., & Allen, J. T. (2007). Large-scale circulation
759 around the Crozet Plateau controls an annual phytoplankton bloom in the Crozet Basin.
760 *Deep-Sea Research Part II: Topical Studies in Oceanography*, 54(18–20), 1915–1929.
761 <https://doi.org/10.1016/j.dsr2.2007.06.012>
- 762 Pollard, R., Sanders, R., Lucas, M., & Statham, P. (2007). The Crozet Natural Iron Bloom and
763 Export Experiment (CROZEX). *Deep-Sea Research Part II: Topical Studies in*
764 *Oceanography*, 54(18–20), 1905–1914. <https://doi.org/10.1016/j.dsr2.2007.07.023>
- 765 Pondaven, P., Fravallo, C., Ruiz-Pino, D., Tréguer, P., Quéguiner, B., & Jeandel, C. (1998).
766 Modelling the silica pump in the Permanently Open Ocean Zone of the Southern Ocean.
767 *Journal of Marine Systems*, 17(1-4), 587-619.
- 768 Pörtner, H. O., Peck, L., & Somero, G. (2007). Thermal limits and adaptation in marine
769 Antarctic ectotherms: An integrative view. *Philosophical Transactions of the Royal*
770 *Society B: Biological Sciences*, 362(1488), 2233–2258.
771 <https://doi.org/10.1098/rstb.2006.1947>

772 Post, A. L., Meijers, A. J. S., Fraser, A. D., Meiners, K. M., Ayers, J., Bindoff, N. ., ...
773 Raymond, B. (2014). Environmental setting. In *Biogeographic Atlas of the Southern*
774 *Ocean* (pp. 418–421).

775 R Core Team. (2018). *R: A language and environment for statistical computing*. Retrieved
776 from <https://www.r-project.org/>

777 Raymond, B. (2014). Pelagic Regionalisation. In *Biogeographic Atlas of the Southern Ocean*,
778 418–421.

779 Reygondeau, G., & Huettmann, F. (2014). Past, present and future state of pelagic habitats in
780 the Antarctic Ocean. *Biogeographic Atlas of the Southern Ocean*, 397–403.

781 Ropert-Coudert, Y., Hindell, M. A., Phillips, R. A., Charrassin, J. B., Trudelle, L., &
782 Raymond, B. (2014). Biogeographic Patterns of Birds and Mammals. In *Biogeographic*
783 *Atlas of the Southern Ocean* (pp. 418–421).

784 Roquet, F., Park, Y. H., Guinet, C., Bailleul, F., & Charrassin, J. B. (2009). Observations of
785 the Fawn Trough Current over the Kerguelen Plateau from instrumented elephant seals.
786 *Journal of Marine Systems*, 78(3), 377–393.
787 <https://doi.org/10.1016/j.jmarsys.2008.11.017>

788 Sanial, V., van Beek, P., Lansard, B., D'Ovidio, F., Kestenare, E., Souhaut, M., ... Blain, S.
789 (2014). Study of the phytoplankton plume dynamics off the Crozet Islands (Southern
790 Ocean): A geochemical-physical coupled approach. *Journal of Geophysical Research:*
791 *Oceans*, 119(4), 2227–2237. <https://doi.org/10.1002/2013JC009305>

792 Sokolov, S., & Rintoul, S. R. (2007). On the relationship between fronts of the Antarctic
793 Circumpolar Current and surface chlorophyll concentrations in the Southern Ocean.

794 *Journal of Geophysical Research: Oceans*, 112(7), 1–17.
795 <https://doi.org/10.1029/2006JC004072>

796 Sokolov, S., & Rintoul, S. R. (2009). Circumpolar structure and distribution of the antarctic
797 circumpolar current fronts: 1. Mean98 circumpolar paths. *Journal of Geophysical*
798 *Research: Oceans*, 114(11), 1–19. <https://doi.org/10.1029/2008JC005108>

799 Spalding, M. D., Fox, H. E., Allen, G. R., Davidson, N., Ferdaña, Z. A., Finlayson, M., ...
800 Robertson, J. (2007). Marine Ecoregions of the World: A Bioregionalization of Coastal
801 and Shelf Areas. *BioScience*, 57(7), 573–583. <https://doi.org/10.1641/B570707>

802 Takahashi, K. T., Kawaguchi, S., Kobayashi, M., Hosie, G. W., Fukuchi, M., & Toda, T.
803 (2002). Zooplankton distribution patterns in relation to the Antarctic Polar Front Zones
804 recorded by Continuous Plankton Recorder (CPR) during 1999/2000 Kaiyo Maru cruise.
805 *Polar Bioscience*, 15, 97–107. <https://doi.org/10.1016/j.polar.2011.04.003>

806 Takahashi, K. T., Hosie, G. W., Kitchener, J. A., McLeod, D. J., Odate, T., & Fukuchi, M.
807 (2010). Comparison of zooplankton distribution patterns between four seasons in the
808 Indian Ocean sector of the Southern Ocean. *Polar Science*, 4(2), 317–331.
809 <https://doi.org/10.1016/j.polar.2010.05.002>

810 Takahashi, K. T., Hosie, G. W., McLeod, D. J., & Kitchener, J. A. (2011). Surface
811 zooplankton distribution patterns during austral summer in the Indian sector of the
812 Southern Ocean, south of Australia. *Polar Science*, 5(2), 134–145.
813 <https://doi.org/10.1016/j.polar.2011.04.003>

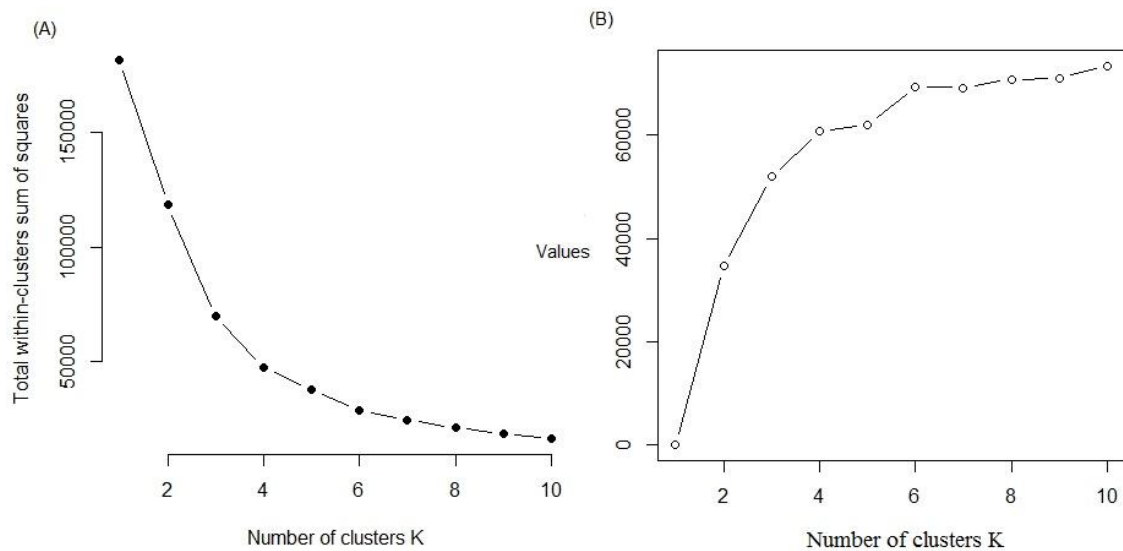
814 Turner, J., Barrand, N. E., Bracegirdle, T. J., Convey, P., Hodgson, D. A., Jarvis, M., ...
815 Klepikov, A. (2014). Antarctic climate change and the environment: an update. *Polar*
816 *Record*, 50(3), 237–259. <https://doi.org/10.1017/S0032247413000296>

817 Venkataramana, V., Anilkumar, N., Naik, R. K., Mishra, R. K., & Sabu, P. (2019).
818 Temperature and phytoplankton size class biomass drives the zooplankton food web
819 dynamics in the Indian Ocean sector of the Southern Ocean. *Polar Biology*, 42(4), 823–
820 829. <https://doi.org/10.1007/s00300-019-02472-w>

821 Appendix

822 **Appendix A.** Outputs of the elbow method (A) and the method of the Calinski Harabasz
823 index (B) which were used was used to choose the optimal number of clusters and determined
824 the 6 bioregions of our study

825



826

827